EPJ Web of Conferences **97**, 00024 (2015)
DOI: 10.1051/epjconf/20159700024

Investigating hadronic resonances in pp interactions with HADES

Witold Przygoda[1,*] for the HADES Collaboration:
J. Adamczewski-Musch[2], O. Arnold[10,9], E.T. Atomssa[15], C. Behnke[8], J.C. Berger-Chen[10,9], J. Biernat[1], A. Blanco[4], C. Blume[8], M. Böhmer[10], P. Bordalo[4], S. Chernenko[7], C. Deveaux[11], A. Dybczak[1], E. Epple[10,9], L. Fabbietti[10,9], O. Fateev[7], P. Fonte[2,a], C. Franco[4], J. Friese[10], I. Fröhlich[8], T. Galatyuk[5,b], J. A. Garzón[17], K. Gill[8], M. Golubeva[12], F. Guber[12], M. Gumberidze[5,b], S. Harabasz[5,1], T. Hennino[15], S. Hlavac[3], C. Höhne[11], R. Holzmann[2], A. Ierusalimov[7], A. Ivashkin[12], M. Jurkovic[10], B. Kämpfer[6,c], T. Karavicheva[12], B. Kardan[8], I. Koenig[2], W. Koenig[2], B. W. Kolb[2], G. Korcyl[1], G. Kornakov[5], R. Kotte[6], A. Krása[16], E. Krebs[8], H. Kuc[3,15], A. Kugler[16], T. Kunz[10], A. Kurepin[12], A. Kurilkin[7], P. Kurilkin[7], V. Ladygin[7], R. Lalik[10,9], K. Lapidus[10,9], A. Lebedev[13], L. Lopes[4], M. Lorenz[8,f], T. Mahmoud[11], L. Maier[10], A. Mangiarotti[4], J. Markert[8], V. Metag[11], J. Michel[8], C. Müntz[8], R. Münzer[10,9], L. Naumann[6], M. Palka[1], Y. Parpottas[14,d], V. Pechenov[2], O. Pechenova[8], V. Petousis[14], J. Pietraszko[2], B. Ramstein[15], L. Rehnisch[8], A. Reshetin[12], A. Rost[5], A. Rustamov[8], A. Sadovsky[12], P. Salabura[1], T. Scheib[8], K. Schmidt-Sommerfeld[10], H. Schuldes[8], P. Sellheim[8], J. Siebenson[10], L. Silva[4], Yu.G. Sobolev[16], S. Spataro[e], H. Ströbele[8], J. Stroth[8,4], P. Strzempek[1], C. Sturm[2], O. Svoboda[16], A. Tarantola[8], K. Teilab[8], P. Tlusty[16], M. Traxler[2], H. Tsertos[14], T. Vasiliev[7], V. Wagner[16], C. Wendisch[6,c], J. Wirth[10,9], J. Wüstenfeld[6], Y. Zanevsky[7], P. Zumbruch[2,a]

[1] *(HADES collaboration)*
[1] *Smoluchowski Institute of Physics, Jagiellonian University of Cracow, 30-348 Kraków, Poland*
[2] *GSI Helmholtzzentrum für Schwerionenforschung GmbH, 64291 Darmstadt, Germany*
[3] *Institute of Physics, Slovak Academy of Sciences, 84228 Bratislava, Slovakia*
[4] *LIP-Laboratório de Instrumentação e Física Experimental de Partículas , 3004-516 Coimbra, Portugal*
[5] *Technische Universität Darmstadt, 64289 Darmstadt, Germany*
[6] *Institut für Strahlenphysik, Helmholtz-Zentrum Dresden-Rossendorf, 01314 Dresden, Germany*
[7] *Joint Institute of Nuclear Research, 141980 Dubna, Russia*
[8] *Institut für Kernphysik, Goethe-Universität, 60438 Frankfurt, Germany*
[9] *Excellence Cluster 'Origin and Structure of the Universe' , 85748 Garching, Germany*
[10] *Physik Department E12, Technische Universität München, 85748 Garching, Germany*
[11] *II.Physikalisches Institut, Justus Liebig Universität Giessen, 35392 Giessen, Germany*
[12] *Institute for Nuclear Research, Russian Academy of Science, 117312 Moscow, Russia*
[13] *Institute of Theoretical and Experimental Physics, 117218 Moscow, Russia*
[14] *Department of Physics, University of Cyprus, 1678 Nicosia, Cyprus*
[15] *Institut de Physique Nucléaire (UMR 8608), CNRS/IN2P3 - Université Paris Sud, F-91406 Orsay Cedex, France*
[16] *Nuclear Physics Institute, Academy of Sciences of Czech Republic, 25068 Rez, Czech Republic*
[17] *LabCAF. F. Física, Univ. de Santiago de Compostela, 15706 Santiago de Compostela, Spain*

[a] *also at ISEC Coimbra, Coimbra, Portugal*

*e-mail: witold.przygoda@uj.edu.pl

[b] also at ExtreMe Matter Institute EMMI, 64291 Darmstadt, Germany
[c] also at Technische Universität Dresden, 01062 Dresden, Germany
[d] also at Frederick University, 1036 Nicosia, Cyprus
[e] also at Dipartimento di Fisica and INFN, Università di Torino, 10125 Torino, Italy
[f] also at Utrecht University, 3584 CC Utrecht, The Netherlands

Abstract. In this paper we report on the investigation of baryonic resonance production in proton-proton collisions at the kinetic energies of 1.25 GeV and 3.5 GeV, based on data measured with HADES. Exclusive channels $np\pi^+$ and $pp\pi^0$ as well as ppe^+e^- were studied simultaneously in the framework of a one-boson exchange model. The resonance cross sections were determined from the one-pion channels for $\Delta(1232)$ and N(1440) (1.25 GeV) as well as further Δ and N^* resonances up to 2 GeV/c^2 for the 3.5 GeV data. The data at 1.25 GeV energy were also analysed within the framework of the partial wave analysis together with the set of several other measurements at lower energies. The obtained solutions provided the evolution of resonance production with the beam energy, showing a sizeable non-resonant contribution but with still dominating contribution of $\Delta(1232)P_{33}$. In the case of 3.5 GeV data, the study of the ppe^+e^- channel gave the insight on the Dalitz decays of the baryon resonances and, in particular, on the electromagnetic transition form-factors in the time-like region. We show that the assumption of a constant electromagnetic transition form-factors leads to underestimation of the yield in the dielectron invariant mass spectrum below the vector mesons pole. On the other hand, a comparison with various transport models shows the important role of intermediate ρ production, though with a large model dependency. The exclusive channels analysis done by the HADES collaboration provides new stringent restrictions on the parameterizations used in the models.

1 Elementary reactions and their description

A path to understanding nuclear forces usually begins with the studies of nucleon-nucleon reactions. High precision measurements and a complete reconstruction of the final state provide invaluable insight into the nature of nucleon-nucleon interactions. These studies have to be performed with increasing energy since new processes are involved above the one-pion and two-pion production thresholds (for a review see [1]). Over the years various approaches were studied within the one-boson exchange (OBE) model (see i.e. [2–7]) successfully describing the data. The OBE potential describing the nucleon-nucleon interaction assumes meson exchange ($\pi, \eta, \rho...$) and introduces free parameters like coupling constants which are adjusted according to the data. For example, excitation of lower lying baryon resonances like $\Delta(1232)$ is realized with various form factor parameterizations. In the model proposed by Suslenko and Gaisak [8], the dominance of the one-pion exchange term was assumed leading to a qualitatively well description of experimental data collected in the energy range 0.6 – 1.0 GeV. The analysis of one-pion production channels in reactions $pp \to pp\pi^0$ and $pp \to np\pi^+$ (see [9–12]) leads to a good description of various differential distributions, yet the total cross sections predicted by the model are lower than the reconstructed from the experimental data. Another model describing the data in the $np\pi^+$ channel in the quite wide energy range 0.97 – 4.0 GeV (see [13–15]), introduced by Dmitriev, Sushkov and Gaarde [16], had essentially similar assumptions of one-pion exchange but different vertex parameterization. It became part of a more versatile resonance model by Teis *et al.* [17] describing the production of mesons in elementary and heavy-ion collisions in the energy range of 1 – 2 GeV/u. The model inherited anisotropic angular description of the Δ resonance

from the OPE model [16] but replaced the parameterization of Δ resonance total width according to the Moniz model [18], highly suppressing the high-mass tail of the Δ resonance. In the case of higher lying resonances, the resonance model [17], like many transport models (i.e. UrQMD [19] and GiBUU [20]), uses the isotropic distributions. The total cross sections is obtained as the incoherent sum of all resonances contributing to a specific channel fixed by the fit to the data on 1π-, η, ρ and 2π production assuming constant matrix elements.

Another approach to the description of one-pion production is a partial wave analysis. The results discussed in this report utilize the framework of the Bonn-Gatchina group. It was successfully applied for the description of $p + p$ data measured at lower beam energies (see [11] and [12]). In the partial wave analysis the total amplitude is described as a sum of partial wave amplitudes with corresponding angular dependencies:

$$A = \sum_{\alpha} A^{\alpha}_{tr}(s) Q^{in}_{\mu_1 \ldots \mu_J}(S, L, J) A_{2b}(j, S_2, L_2, J_2)(s_i) \times Q^{fin}_{\mu_1 \ldots \mu_J}(i, S_2, L_2, J_2, S', L', J), \tag{1}$$

where S, L, J are spin, orbital momentum and total angular momentum of the initial NN system, S_2, L_2, J_2 are spin, orbital momentum and total angular momentum of the two-particle system in the final state and S', L' are spin and orbital momentum between this two-particle system and the spectator particle with index j. The invariant mass of two-body system is defined by $s_j = (P - q_j)^2$ where q_j is the four-momentum of the spectator and P is the total momentum of the reaction. The operators Q^{in} and Q^{fin} are tensors constructed for each event from the momenta of the initial and the final particles. Their explicit form is given in [21]. For the transition amplitude from initial NN to $NN\pi$ system A^{α}_{tr} we introduced the multi-index α which summarizes all quantum numbers described above, in the same form as it was done in [11, 12]:

$$A^{\alpha}_{tr} = \frac{a^{\alpha}_1 + \sqrt{s}\, a^{\alpha}_3}{s - s^{\alpha}_0} e^{i a^{\alpha}_2}, \tag{2}$$

where $a^{\alpha}_1, a^{\alpha}_2, a^{\alpha}_3$ and s^{α}_0 are real numbers and the poles at $s = s^{\alpha}_0$ are located in the region of left-hand side singularities of the partial wave amplitudes. The A_{2b} contribution for resonance production in the πN channel was parameterized as relativistic Breit-Wigner amplitudes (for the exact form, see e.g. [11]). Although it is not equivalent to a parameterization used in the resonance model (the above mentioned Moniz parameterization), at the proton kinetic energy of 1.25 GeV the data are not very sensitive for the resonance parameterization. The masses and total widths of the resonances were taken from the Particle Data Group [22] and fixed in the fit. The non-resonant A_{2b} contributions in the NN scattering channel were parameterized with a modified scattering length approximation (see [11]), which corresponds exactly to the scattering-length formula from [23, 24] in the case of S-waves. There, the pn scattering length and effective range were fixed at $a(^1S_0) = -23.7$ fm, $r(^1S_0) = 2.8$ fm and $a(^3S_1) = 5.3$ fm, $r(^3S_1) = 1.8$ fm. In most of the fits, the only fitted function was the transition amplitude $A^{\alpha}_{tr}(s)$. The differential cross section calculated for this amplitude is maximized with the event-by-event maximum likelihood method, which takes into account all correlations in the multidimensional phase space. The solution is based on the simultaneous fit to many experimental data samples, with the energy dependence (see Eq. 2). The resulting cross section is the coherent sum of both resonant and non-resonant contributions within a given initial partial wave.

An experimentally demanding but powerful way to explore the electromagnetic structure of baryon resonances (R) is the study of their decay into a nucleon and a massive virtual photon converting into dilepton pair, so called Dalitz decay. The description of interaction vertex $NR\gamma^*$ by electromagnetic transition form factors (eTFF) is also challenging theoretically, since in the time-like region ($q^2 > 0$, q is the four-momentum transfer) it is strongly influenced by vector meson-poles. This can

be experimentally probed by measurements of the resonance Dalitz decays (Ne^+e^-) and indeed, many theoretical calculations predict significant effects on the resulting dilepton invariant mass distribution due to vector mesons (ρ/ω). The famous vector meson dominance (VMD) model by Sakurai [25] couples the virtual photon to a hadron by the intermediate vector meson fields. However, such couplings lead to an overestimate of the radiative $R \to N\gamma$ decay widths when the known $R \to N\rho$ branching ratios are used in calculations, and various ideas to overcome this conflict have been used e.g. separate $N\gamma$ and $N\rho$ couplings [26], or destructive interferences between contributions from higher ρ/ω states [27] or different forms of the eTFF for the quark and the pion cloud coupling [28]). On the other hand, such models should be effectively anchored in the space-like region ($q^2 < 0$) where a rich data sample on the eTFF for the $\Delta(1232)$, N(1440) and N(1520) has been obtained in a wide q^2 range (for a review see [29]). To clarify the question about resonance production and the prominent role of the coupling to ρ, the exclusive data are necessary.

In this work we discuss the results from the exclusive hadronic channels $pp \to np\pi^+$, $pp \to pp\pi^0$ investigated at the kinetic beam energies of 1.25 and 3.5 GeV and a dilepton channel $pp \to ppe^+e^-$ investigated at the kinetic beam energy of 3.5 GeV.

2 HADES experiments

The High Acceptance Di-Electron Spectrometer (HADES) [30] is installed at the GSI Helmholtzzentrum für Schwerionenforschung in Germany. In two of the experiments a proton beam of 10^7 particles/s with kinetic energy of 1.25 GeV or 3.5 GeV was impinging on a liquid-hydrogen target. The details about the track reconstruction and particle identification were described in [31, 32]. All spectra were normalized to the $p + p$ elastic scattering yield measured within the same experimental runs (for details, see [31, 33]). The normalization error was estimated to be 8% in both cases. To study one-pion production mechanisms events with one proton and one pion ($p\pi^+$) and two protons (pp) were selected. For the ppe^+e^- final state, events containing at least one proton track and one e^+e^- pair were selected. The subsequent final states were identified via cuts in the one-dimensional missing mass distributions around the value of the not detected particle, e.g. neutron, π^0 or proton, respectively. The momentum vectors of not detected particles were obtained from momentum conservation. The background estimation in hadronic channels was done with the help of missing mass spectrum plotted at various parts of the two-dimensional $cos\theta^{CM}_{p\pi^+}$ vs $M^{inv}_{p\pi^+}$ representation. Prior to the background evaluation, the two-pion contribution was subtracted in the missing mass spectrum, then the fitting of the signal peak and various forms (polynomials) of the background were used to study systematics. In dilepton channels, the combinatorial background (CB) was estimated using the like-sign pair technique (given as a sum of like-sign pairs), as described in [30, 31].

3 One-pion channels at 1.25 GeV

At the 1.25 GeV kinetic energy of the proton beam, the dominant contribution in the $pp \to np\pi^+$ channel stems from the intermediate Δ^{++} resonance. Comparison to the OPE model [16] requires an adjustment of the cut-off parameter Λ_π in the vertex form factor:

$$F(t) = \frac{\Lambda_\pi^2 - m_\pi^2}{\Lambda_\pi^2 - t} \tag{3}$$

where t is the square of the four-momentum of the virtual pion and m_π^2 is the pion mass squared. The HADES data favour $\Lambda_\pi = 0.75$ GeV (see [31]). Further improvement was done with the parameterization correction of the OPE model based on the two-dimensional $cos\theta^{CM}_{p\pi^+}$ vs $M^{inv}_{p\pi^+}$ representation,

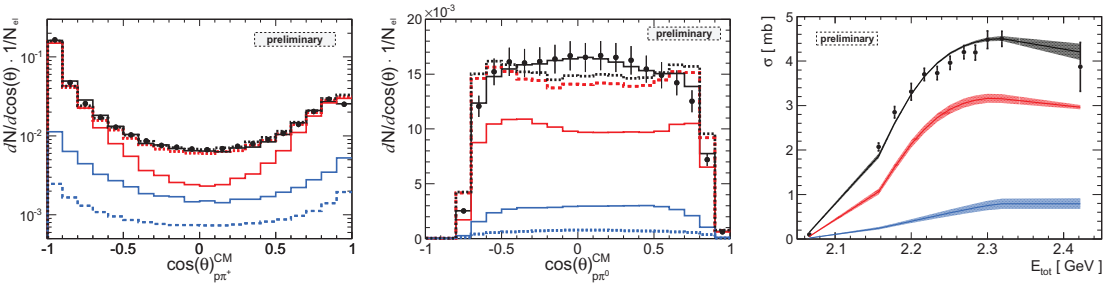

Figure 1. Uncorrected angular distributions of the $p\pi^+$ (left, notice the log scale) and $p\pi^0$ (middle, in linear scale) system in the CM frame within the acceptance of the HADES spectrometer, normalized to the number of pp elastic reactions (N_{el}). The total partial wave analysis (PWA) solution (black curve) with the resonance components, red curve - $\Delta(1232)P_{33}$ contribution, blue curve - $N(1440)P_{11}$ contribution is compared to the modified OPE model (dashed curves, the same color code). Right: cross section of the $pp\pi^0$ channel (12 data points) and the PWA solution (black curve) decomposed into intermediate resonances $\Delta(1232)$ (red curve) and N(1440) (blue curve). The shaded bands represent the systematic uncertainties of the PWA solution.

adjusted to the experimental data. The feasibility of the model modification is exampled in Fig. 1 left, where the angular distribution of the $p\pi^+$ system in the CM frame within the HADES acceptance is compared to the Monte-Carlo model simulation (dashed curves) in the log scale. Based on the good model description and good acceptance coverage, the data were acceptance and efficiency corrected, resulting in the total cross section 17.00 ± 2.2 mb for the $np\pi^+$ channel. The systematic error includes the uncertainties due to particle identification, background subtraction, normalization error and the correction uncertainty. The modified OPE model was applied to the Δ^+ production in the $pp\pi^0$ channel. The identification of two protons in the HADES acceptance results in the limited inelastic reaction acceptance, covering high four-momentum transfer. Although slight discrepancies between the data and the model, i.e. in the angular projection of the $p\pi^0$ system in CM frame, are still present (see Fig. 1 middle, dashed curves) the overall agreement is good. The acceptance correction of the data with the model-driven extrapolation results in 3.87 ± 0.55 mb of the cross section for the $pp\pi^0$ channel.

Although the corrected OPE model describes acceptably well the angular and mass distributions and can be used for the acceptance correction of the data it does not provide a fully physical understanding of the data and the role of other contributions which are not connected with the Δ production are introduced in a very simplified form. Therefore, the partial wave analysis of the Bonn-Gatchina group was enforced, starting from the solution found in [11]. The analysis was performed including other available data sets (see [34], eleven measurements for $pp\pi^0$ and two for the $pn\pi^+$ channel) covering mostly lower beam energies. For the proper HADES data description, high partial waves are necessary, which contribute to the forward/backward peaked parts of the angular distributions of the $p\pi^+$ and $p\pi^0$ systems in the CM frame. Various solutions were investigated based on parameterizations of the transition amplitude A_{tr} (Eq. 2) and descriptions of resonance states (Δ and in particular, N^*). The obtained solutions generally describe the HADES data very well in various projections (Fig. 1 left and middle, black solid curve). The analysis shows the dominant $\Delta(1232)P_{33}$ contribution in $np\pi^+$ at the level of 75% (see Fig. 1 right, red band), stemming from the ${}^3P_2$, ${}^3P_1$ and ${}^3F_4$ incoming partial waves. It results in the total cross section 16.4 ± 0.8 mb (model systematic error). In the case of $pp\pi^0$, the intermediate $\Delta(1232)P_{33}$ state amounts 70% from the ${}^3P_2$, ${}^3F_4$ and ${}^3F_2$ as the major con-

tributors and the extracted cross section is 4.2 ± 0.15 mb. The N(1440)P_{11} contribution is noticeably higher than in the resonance model, and reaches several percent (12% for $np\pi^+$ and 20% for $pp\pi^0$ channel, see Fig. 1 right, blue band). The partial wave solutions include also notable interferences between non-resonant contributions and the N(1440) channel resulting in the larger systematic error on initial partial waves contribution. Based on the multidimensional PWA solution the acceptance correction can be done as in the resonance model case. The obtained cross sections are very close to the PWA solution prediction but with larger systematic errors (16.3 ± 2.0 mb for the $np\pi^+$ channel and 4.1 ± 0.45 mb for the $pp\pi^0$ channel).

4 One-pion channels at 3.5 GeV

At 3.5 GeV kinetic energy of the proton beam the one-pion channels involve the decays of Δ and N^* resonances with masses up to 2 GeV/c^2. Starting the description with the resonance model [17] one has to recall that the resonance with the anisotropic angular distribution is the Δ(1232), based on OPE calculation [16]. The separation of the double (Δ^{++}) and the single charged resonances (Δ^+, N^{*+}) by the analysis of the $p\pi^+$ and the $n\pi^+$ invariant mass distributions is feasible. Further procedure utilizes parameterizations of the higher mass resonances taken from the Teis *et al.* model [17] but production yields and the angular distributions are treated as free parameters. The latter one is assumed to be governed by the t dependency:

$$d\sigma_R/dt \propto A/t^{\alpha} \tag{4}$$

where t is the four-momentum transfer squared, calculated between the four-momentum vectors of the outgoing resonance and the incoming nucleon, A and α are constants to be derived from the comparison to the data. The yields of the resonances were obtained from simultaneous fits to the invariant mass and the four-momentum transfer distributions in the iterative procedure described in [32]. Although the identification of resonances is ambiguous in the nucleon-pion invariant mass region of overlapping states, the decomposition is still feasible. It is performed by a comparison of the corresponding yields in the $n\pi^+$ and $p\pi^+$ invariant mass distributions for the N^* and Δ resonances and is given as the product of the resonance cross section and the respective branching ratio. The decomposition of the simulated $p\pi^+$ yields was also tested as a function of $cos(\theta)^{CM}_{p\pi^+}$. Finally, the extracted resonance yields and the angular distributions were included in the simulation of the $pp \rightarrow pp\pi^0$ reaction channel. The cross sections for the $pn\pi^+$ and $pp\pi^0$ final states are fixed by their isospin relations and an agreement between simulation and the data was also achieved for this reaction channel. The feasibility of the obtained multi-resonance fit was also tested on comparisons between the data and the angular distributions defined in the Gottfried-Jackson and the helicity reference frames. The modified resonance model can be used for the acceptance correction of the data (Fig. 2, black dots). The obtained cross sections can be then compared to the values predicted by the resonance model [17], but also other parametrization used, e.g. on GiBUU [20, 35] and UrQMD [19]. The detailed results are discussed in [32]. They are presented in Fig. 2 (lower row pictures with invariant masses of $p\pi^+$ and $n\pi^+$). The $\Delta(1232)^+$ cross section obtained in the HADES analysis is slightly higher than that of the resonance model [17] and GiBUU [35]. The total contribution of higher mass Δ resonances is lower than in the fit of [17] but in line with the cross sections applied in the GiBUU version [35]. On the other hand the higher mass Δ resonances are by a factor 2-3 larger in the UrQMD code [19] but lower for the Δ(1232). For the N^* the cross sections of N(1440), N(1520) and N(1535) can be studied directly. The constraint on the N(1535) production comes from the analysis of the $pp\eta$ Dalitz plot with η decaying into $\pi^0\pi^+\pi^-$ identified in the same measurement [36]. The contribution of this reaction channel amounts to about 47% leading to the total production cross section $\sigma_{N(1535)} \simeq 0.157$ mb when taking into account the BR($N(1535) \rightarrow N\eta$) = 0.42 [22]. The parametrization used in the

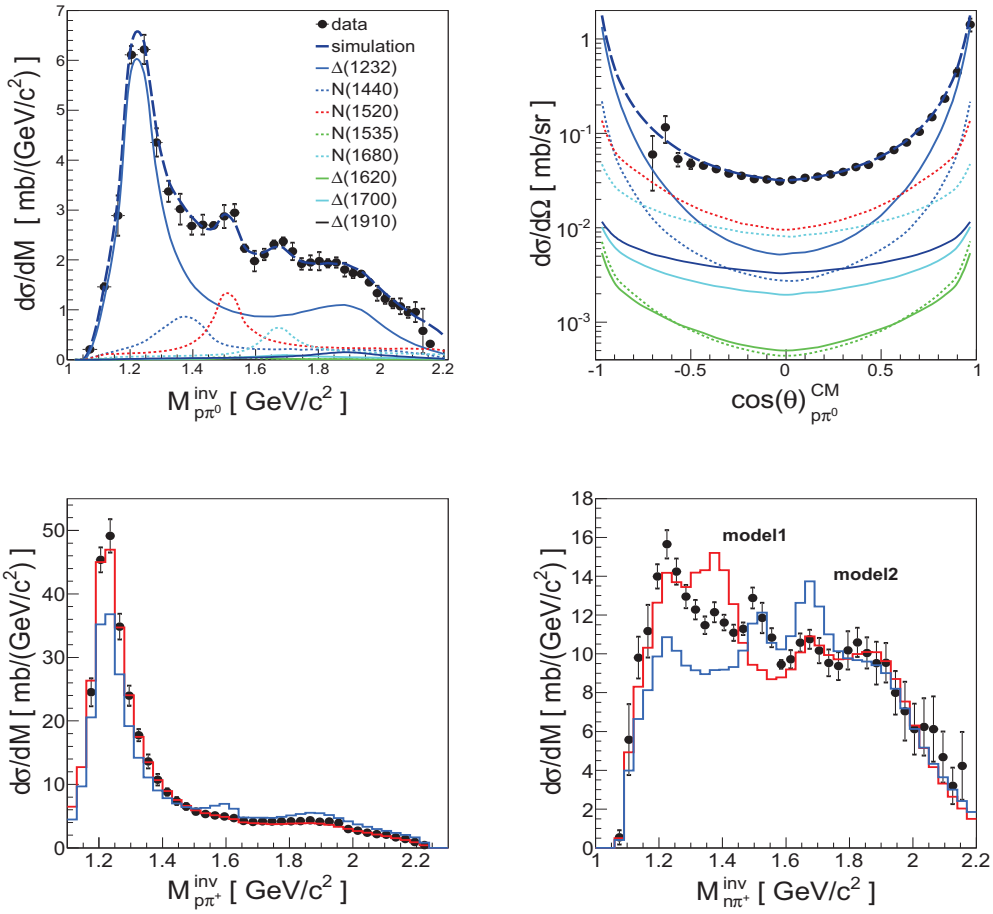

Figure 2. Upper row pictures: $pp\pi^0$ final state. Acceptance corrected $p\pi^0$ invariant mass and the CM angular distributions (black dots) compared to the simulation result (dashed curves). Resonance contributions are shown separately (line style described in the legend). Lower row pictures: $np\pi^+$ final state. Acceptance corrected $p\pi^+$ and $n\pi^+$ invariant mass distributions (black dots) compared to the simulation results using the resonance cross sections according to parameterization taken from the GiBUU [35] (red curve - *model*1) or from the UrQMD [19] (blue curve - *model*2).

transport models use much larger N(1535) cross sections: 0.53 mb (GiBUU) and 0.8 mb (UrQMD). GiBUU gives the largest weight to the N(1440) and a smaller one to the N(1675). The cross sections for N(1720) and N(1680) used in UrQMD [19] are much higher than the ones used in GiBUU [35]. In view of such discrepancies, even more constraints can be provided by the exclusive analysis of the dilepton channels.

5 Dilepton channels at 3.5 GeV

The $pp e^+e^-$ final state was selected by a cut on the pe^+e^- missing mass 0.8 GeV/c^2 < $M^{miss}_{pe^+e^-}$ < 1.04 GeV/c^2. This distribution and the e^+e^- and the pe^+e^- invariant mass distributions are used in comparison to various models. All experimental distributions were normalized to the measured

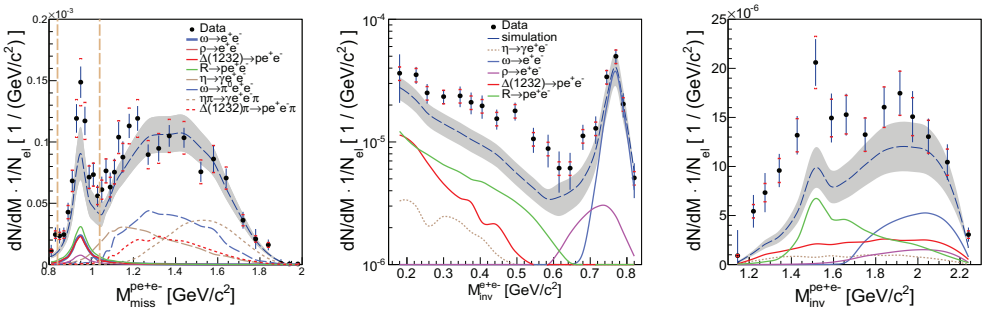

Figure 3. ppe^+e^- final state: pe^+e^- missing mass (left), dielectron (middle) and pe^+e^- (right) invariant mass distributions compared to the simulation result assuming a point-like $RN\gamma^*$ coupling [39]. The error bars represent statistical (black) and the normalization (red) errors. The invariant mass distributions have been obtained for events inside the indicated window (vertical dashed lines in the left panel) on the pe^+e^- missing mass. The hatched area indicates the model errors (for more details see text). Number of counts is per mass bin width.

elastic scattering yields (Sec. 2) and the simulation results were filtered through the acceptance and efficiency matrices followed by a smearing with the experimental resolution. The simulations assume the production cross sections σ_R of baryon resonances deduced in the channels with one pion, as described in Section 4 and [32]. Besides, the total cross sections of the exclusive η and ω production, $\sigma_\eta = 140 \pm 14\ \mu b$, $\sigma_\omega = 146 \pm 15\ \mu b$, respectively, were obtained from a parametrization of the existing data [31, 37]. The total cross section for ρ meson production was obtained from the ω cross section by $\sigma_{pp\rho} = 0.5\sigma_{pp\omega}$, as observed at $E_{beam} = 2.85$ GeV in the DISTO experiment [38].

The comparison to the model [39], which assumes constant eTFF and a point-like $RN\gamma^*$ coupling, establishes lower limits for the e^+e^- emission. The missing mass distribution of the pe^+e^- system is shown in Fig. 3 (left). The distribution is compared with the result of the simulation (dashed curve) including the baryon resonances and ρ, ω and η meson sources. The baryon resonances were grouped into two contributions, originating from the $\Delta(1232)$ and the higher mass (Δ^+, N^*) states. The hatched area covers the model uncertainties related to the errors of resonance and meson production cross sections. A description of the pe^+e^- missing mass distribution could be achieved with all the sources, except for the yield in the proton missing-mass peak itself (for the discussion, see [32]). The background under the proton peak, related to final states other than ppe^+e^-, is smaller than 6%. The middle part of Fig. 3 displays the e^+e^- invariant mass distribution for the events within the pe^+e^- missing mass window. It is compared to the simulation including dielectron sources originating from the baryon resonance decays and the two-body meson ρ, $\omega \rightarrow e^+e^-$ decays. The agreement in the vector mass pole verifies also that the normalization and the simulations of the HADES acceptance and reconstruction efficiencies are under control. On the other hand, an excess of the contributions from the baryon resonances is visible below the vector meson pole. The effect is related to the excess in the proton missing-mass window and can be explained by the contributions from off-shell couplings of the resonances to the vector mesons. Such couplings should modify the respective eTFF which were assumed to be constant in the simulations. The comparison of the pe^+e^- invariant mass distribution with the simulation displayed in Fig. 3 (right) shows that the excess is indeed located around the N(1520) resonance, known to have a sizeable decay branch to the ρ meson.

6 Summary

The HADES data measured for the pion production reactions in proton-proton collision were analyzed with a modified OPE resonance model [17] and with the Bonn-Gatchina [21] partial wave analysis method (for 1.25 GeV, the analysis of 3.5 GeV data is on-going). The results of OPE calculations and the obtained PWA solution allowed us to perform a full phase space acceptance correction of the measured data and to deduce the total cross sections of resonance contribution. The comparison to transport models, like the GiBUU [20] and UrQMD [19], unraveled many discrepancies. In the dilepton channel (3.5 GeV), upper limits for the various resonance contributions have been obtained assuming point-like baryon-virtual-photon couplings. The calculated dielectron yields cannot reproduce the measured yield and suggest strong off-shell vector meson couplings, which should influence the respective electromagnetic transition form-factors. Another approach for the Dalitz decay of resonances can be studied within the transport models (GiBUU [20, 35], UrQMD [19]), since they implement the scheme of a two step factorization $R \to p\rho \to pe^+e^-$ in the dilepton production. It turns out that not only resonance cross sections (as discussed in Sec. 4) but also the resonance-ρ couplings are different, also when compared to the newest multichannel partial wave analyses e.g. the newest Shrestha and Manley calculations [40], Bonn-Gatchina group [41] or the CLAS collaboration [42] results (for the discussion, see [32]). The discrepancies call for further efforts, both on experimental and theoretical sides. The recently measured pion-proton collisions with the HADES spectrometer should deliver valuable information on the resonance excitation and coupling to virtual photons.

Acknowledgements

The authors kindly thank A. V. Sarantsev for the collaboration in the partial wave analysis. The HADES Collaboration gratefully acknowledges the support by the grants: PTDC/FIS/113339/2009 LIP Coimbra, NCN grant 2013/10/M/ST2/00042 SIP JUC Cracow, Helmholtz Alliance HA216/EMMI GSI Darmstadt, VH-NG-823, Helmholtz Alliance HA216/EMMI TU Darmstadt, 283286, 05P12CRGHE HZDR Dresden, Helmholtz Alliance HA216/EMMI, HIC for FAIR (LOEWE), GSI F&E Goethe-University, Frankfurt VH-NG-330, BMBF 06MT7180 TU München, Garching BMBF:05P12RGGHM JLU Giessen, Giessen UCY/3411-23100, University Cyprus CNRS/IN2P3, IPN Orsay, Orsay MSMT LG 12007, AS CR M100481202, GACR 13-06759S NPI AS CR, Rez, EU Contract No. HP3-283286.

References

[1] P. Moskal *et al.*, Prog. Part. Nucl. Phys. **49**, 1 (2002).
[2] A. Gersten, R. H. Thompson and A. E. S. Green, Phys. Rev. D **3**, 2076 (1971).
[3] R. A. Bryan and A. Gersten, Phys. Rev. D **6**, 341 (1972); Phys. Rev. D **7**, 2802 (1973).
[4] G. Schierholz, Nucl. Phys. B **40**, 335 (1972).
[5] K. Erkelenz, Phys. Rep. **13C**, 191 (1974).
[6] K. Holinde and R. Machleidt, Nucl. Phys. A **247**, 495 (1975); Nucl. Phys. A **256**, 479 (1976).
[7] R. Machleidt, K. Holinde, and Ch. Elster, Phys. Rep. **149**, 1 (1987).
[8] V. K. Suslenko and I. I. Gaisak, Yad. Fiz. **43**, 392 (1986).
[9] V. P. Andreev, A. V. Kravtsov, M. M. Makarov, V. I. Medvedev, V. I. Poromov, V. V. Sarantsev, S. G. Sherman, G. L. Sokolov and A. B. Sokornov, Phys. Rev. C **50**, 15 (1994).
[10] V. V. Sarantsev, K. N. Ermakov, V. I. Medvedev, T. S. Oposhnyan, O. V. Rogachevsky and S. G. Sherman, Eur. Phys. J. A **21**, 303 (2004).

[11] K. N. Ermakov, V. I. Medvedev, V. A. Nikonov, O. V. Rogachevsky, A. V. Sarantsev, V. V. Sarantsev and S. G. Sherman, Eur. Phys. J. A **50**, 98 (2014).
[12] K. N. Ermakov, V. I. Medvedev, V. A. Nikonov, O. V. Rogachevsky, A. V. Sarantsev, V. V. Sarantsev and S. G. Sherman, Eur. Phys. J. A **47**, 159 (2011).
[13] D. V. Bugg, A. J. Oxley, J. A. Zoll, J. G. Rushbrooke, V. E. Barnes, J. B. Kinson, W. P. Dodd, G. A. Doran, and L. Riddiford, Phys. Rev. **133**, B1017 (1964).
[14] A. M. Eisner, E. L. Hart, R. I. Louttit, and T. W. Morris, Phys. Rev. **138**, B670 (1965).
[15] S. Coletti, J. Kidd, L. Mandelli, V. Pelosi, S. Ratti, V. Russo, L. Tallone, E. Zampieri, C. Caso, F. Conte, M. Dameri, C. Grosso and G. Tomasini, Nuovo Cim. A **49**, 479 (1967).
[16] V. Dmitriev, O. Sushkov, C. Gaarde, Nucl. Phys. A **459**, 503 (1986).
[17] S. Teis, W. Cassing, M. Effenberger, A. Hombach, U. Mosel and G. Wolf, Z. Phys. A **356**, 421 (1997).
[18] J. H. Koch, E. J. Moniz and N. Ohtsuka, Ann. of Phys. **154**, 99 (1984).
[19] S. A. Bass, M. Belkacem, M. Bleicher, M. Brandstetter, L. Bravina, C. Ernst, L. Gerland, M. Hofmann, S. Hofmann, J. Konopka, G. Mao, L. Neise, S. Soff, C. Spieles, H. Weber, L. A. Winckelmann, H. Stöcker, W. Greiner, Ch. Hartnack, J. Aichelin and N. Amelin, Prog. Part. Nucl. Phys. **41**, 255 (1998).
[20] O. Buss, T. Gaitanos, K. Gallmeister, H. van Hees, M. Kaskulov, O. Lalakulich, A. B. Larionov, T. Leitner, J. Weil and U. Mosel, Phys. Rept. **512**, 1 (2012).
[21] A. V. Anisovich, V. V. Anisovich, E. Klempt, V. A. Nikonov and A. V. Sarantsev, Eur Phys. J. A **34**, 129 (2007).
[22] K. A. Olive *et al.* (Particle Data Group), Chin. Phys. C **38**, 090001 (2014).
[23] K. M. Watson, Phys. Rev. **88**, 1163 (1952).
[24] A. B. Migdal, JETP **1**, 2 (1955).
[25] J. J. Sakurai, Ann. Phys. **1**, 1 (1960).
[26] N. M. Kroll, T. D. Lee and B. Zumino, Phys. Rev. **157**, 1376 (1960).
[27] M. I. Krivoruchenko, B. V. Martemyanov, Ann. Phys. **296**, 299 (2002).
[28] G. Ramalho and M. T. Peña, Phys. Rev. D **85**, 113014 (2012).
[29] I. G. Aznauryan and V. D. Burkert, Prog. Part. Nucl. Phys. **67**, 1 (2012).
[30] G. Agakishiev *et al.* (HADES), Eur. Phys. J. A **41**, 243 (2009).
[31] G. Agakishiev *et al.* (HADES), Eur. Phys. J. A **48**, 74 (2012).
[32] G. Agakishiev *et al.* (HADES), Eur. Phys. J. A **50**, 82 (2014).
[33] G. Agakishiev *et al.* (HADES), Eur. Phys. J. A **48**, 64 (2012).
[34] Data Base in http://pwa.hiskp.uni-bonn.de/
[35] J. Weil, H. van Hees and U. Mosel, Eur. Phys. J. A **48**, 111 (2012).
[36] K. Teilab, "The production of eta and omega mesons in 3.5 GeV p+p interaction in HADES" - PhD Thesis, University of Frankfurt (2012).
[37] M. Abdel-Bary *et al.* (COSY-TOF), Eur. Phys. J. A **44**, 7 (2010).
[38] F. Balestra *et al.* (DISTO), Phys. Rev. Lett. **89**, 092001 (2002).
[39] M. Zetenyi and Gy. Wolf., Heavy Ion Phys. **17**, 27 (2003).
[40] M. Shrestha and D. M. Manley, Phys Rev. C **86**, 055203 (2012).
[41] A. V. Anisovich, R. Beck, E. Klempt, V. A. Nikonov, A. V. Sarantsev and U. Thoma, Eur. Phys. J. A **48**, 15 (2012).
[42] V. Mokeev *et al.* (CLAS), Phys Rev. C **86**, 035203 (2012).